Quantum Critical Transport Near the Mott Transition

H. Terletska,[1] J. Vučičević,[2] D. Tanasković,[2] and V. Dobrosavljević[1]

[1]*Department of Physics and National High Magnetic Field Laboratory, Florida State University, Tallahassee, Florida 32306, USA.*
[2]*Scientific Computing Laboratory, Institute of Physics Belgrade, University of Belgrade, Pregrevica 118, 11080 Belgrade, Serbia.*

We perform a systematic study of incoherent transport in the high temperature crossover region of the half-filled one-band Hubbard model. We demonstrate that the family of resistivity curves displays characteristic quantum critical scaling of the form $\rho(T,\delta U) = \rho_c(T) f(T/T_o(\delta U))$, with $T_o(\delta U) \sim |\delta U|^{z\nu}$, and $\rho_c(T) \sim T$. The corresponding β-function displays a "strong coupling" form $\beta \sim \ln(\rho_c/\rho)$, reflecting the peculiar mirror symmetry of the scaling curves. This behavior, which is surprisingly similar to some experimental findings, indicates that Mott quantum criticality may be acting as the fundamental mechanism behind the unusual transport phenomena in many systems near the metal-insulator transition.

PACS numbers: 71.27.+a,71.30.+h

Many systems close to the metal-insulator transition (MIT) often display surprisingly similar transport features in the high temperature regime [1–3]. Here, the family of resistivity curves typically assumes a characteristic "fan-shaped" form (see Fig. 1(a)), reflecting a gradual crossover from metallic to insulating transport. At the highest temperatures the resistivity depends only weakly on the control parameter (concentration of charge carriers [1], or pressure [2, 3]), while as T is lowered, the system seems to "make up its mind" and rapidly converges towards either a metallic or an insulating state. Since temperature acts as a natural cutoff scale for the metal-insulator transition, such behavior is precisely what one expects for quantum criticality [4]. In some cases [1], the entire family of curves displays beautiful scaling behavior, with a remarkable "mirror symmetry" of the relevant scaling functions [4]. But under which microscopic conditions should one expect such scaling phenomenology? What is the corresponding driving force for the transitions? Despite recent progress, such basic physics questions remain the subject of much ongoing controversy and debate.

The phenomenon of disordered-driven Anderson localization of noninteracting electrons is at present rather well understood based on the scaling formulation [5], and is generally viewed as an example of a $T = 0$ quantum phase transition (QPT). On the other hand, a considerable number of recent experiments [1] provide compelling evidence that strong correlation effects - some form of Mott localization - may be the dominant mechanism [6]. Should one expect similar or very different transport phenomenology in the Mott picture? Is the paradigm of quantum criticality even a useful language to describe high temperature transport around the Mott point? These issues are notoriously difficult to address, because conventional Fermi liquid concepts simply cannot be utilized in the relevant high temperature *incoherent* regime. In this Letter we answer this question in the framework of dynamical mean-field theory (DMFT) [1], the only theoretical method that is most reliable precisely at high temperatures.

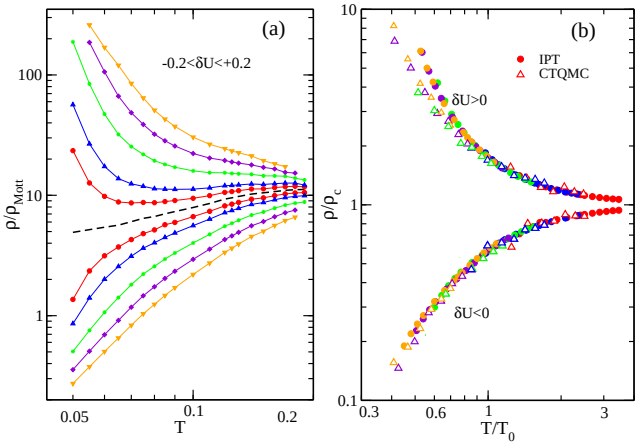

Figure 1: (Color online) (a) DMFT resistivity curves as function of temperature along different trajectories $-0.2 \leq \delta U \leq +0.2$ with respect to the instability line $\delta U = 0$ (black dashed line, see the text). Data are obtained using IPT impurity solver. (b) Resistivity scaling; essentially identical scaling functions are found from CTQMC (open symbols) and from IPT (closed symbols)

Model and DMFT solution. We consider a single-band Hubbard model at half-filling

$$H = -\sum_{<i,j>\sigma} t_{ij}\left(c^\dagger_{i\sigma}c_{j\sigma} + c.c.\right) + \sum_i U n_{i\uparrow}n_{i\downarrow}, \qquad (1)$$

where $c^\dagger_{i\sigma}$ and $c_{i\sigma}$ are the electron creation and annihilation operators, $n_{i\sigma} = c^\dagger_{i\sigma}c_{i\sigma}$, t_{ij} is the hopping amplitude, and U is the repulsion between two electrons on the same site. We use a semicircular density of states, and the corresponding half-bandwidth D is set to be our energy unit. We focus on the paramagnetic DMFT solution, which is formally exact in the limit of large coordination. Here the Hubbard model maps onto an ef-

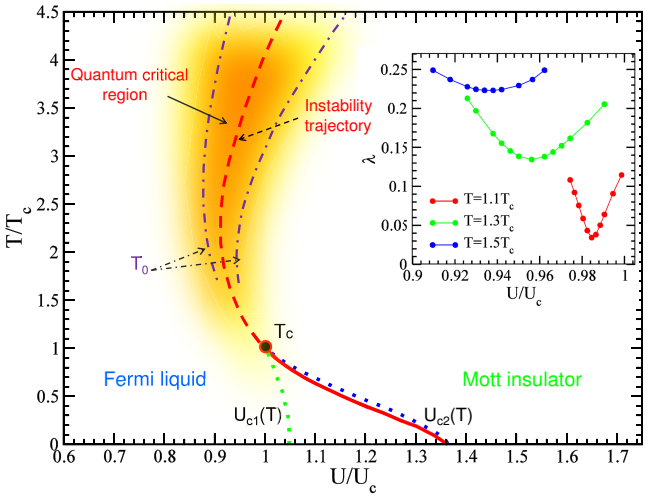

Figure 2: (Color online) DMFT phase diagram of the fully frustrated half-filled Hubbard model, with a shaded region showing where quantum critical-like scaling is found. Metallic $U_{c2}(T)$ and insulating $U_{c1}(T)$ spinodals (dotted lines) are found at $T < T_c$; the corresponding first order phase transition is shown by a thick solid line. The thick dashed line, which extends at $T > T_c$ shows the "instability trajectory" $U^\star(T)$, and the crossover temperature T_o delimits the QC region (dash-dotted lines). The inset shows examples of eigenvalue curves at three different temperatures, with pronounced minima at $U^\star(T)$ determining the instability trajectory.

fective Anderson impurity model supplemented by a self-consistency condition [1]. To solve the DMFT equations we use the iterated perturbation theory (IPT) [1] and cross-check our results with numerically exact continuous time quantum Monte Carlo (CTQMC) [8, 9]. We find, in agreement with previous work [3], that after appropriate energy rescaling (see below), the two methods produce qualitatively and even quantitatively identical results in the incoherent crossover region that we examine.

It is well known that at very low temperatures $T < T_c \sim 0.03$, this model features a first order metal-insulator transition terminating at the critical end-point T_c (Fig. 2), very similar to the familiar liquid-gas transition [3]. For $T > T_c$, however, different crossover regimes have been tentatively identified [1, 11] but they have not been studied in any appreciable detail. The fact that the first order coexistence region is restricted to such very low temperatures provides strong motivation to examine the high temperature crossover region from the perspective of "hidden quantum criticality". In other words, the presence of a coexistence dome at $T < T_c \ll 1$, an effect with very small energy scale, is not likely to influence the behavior at much higher temperatures $T \gg T_c$. In this high temperature regime smooth crossover is found, which may display behavior consistent with the presence of a "hidden" quantum critical (QC) point at $T = 0$. To test this idea, we utilize *standard* scaling methods appropriate for quantum criticality, and compute the resistivity curves along judiciously chosen trajectories respecting the symmetries of the problem.

Instability trajectory formalism. Previous work has already recognized [3] that, in order to reveal the proper scaling behavior close to the critical end-point, one has to follow a set of trajectories parallel to "zero field" trajectory $U^*(T)$. We thus expect $\delta U \equiv U - U^\star(T)$ to play the role of the scaling variable corresponding to a symmetry-breaking field favoring one of the two competing (metal vs. insulator) phases. By analogy [3, 12] to the familiar liquid-gas transition, we determine the precise location of such an "instability trajectory" by examining the curvature of the corresponding free energy functional [13]. This curvature vanishes at T_c and is finite and *minimal* at $T > T_c$, along this instability line. Consequently, as in Refs. [3, 13, 14], our problem is recast as an eigenvalue analysis of the corresponding free energy functional $\mathcal{F}[G(iw_n)]$ for which the DMFT Green's function solution $G_{DMFT}(iw_n)$ represents a local extremum, and can be regarded as a vector in an appropriate Hilbert space.

The free energy near such an extremum can be written as $\mathcal{F}[G(iw_n)] = \mathcal{F}_0 + Tt^2 \sum_{m,n} \delta G(i\omega_m) M_{mn} \delta G(i\omega_n) + \ldots$, where

$$M_{mn} = \frac{1}{2Tt^2} \left. \frac{\partial^2 \mathcal{F}[G]}{\partial G(i\omega_m) \partial G(i\omega_n)} \right|_{G=G_{DMFT}} \qquad (2)$$

and $\delta G(i\omega_n) \equiv G(i\omega_n) - G_{DMFT}(i\omega_n)$. The curvature of the free energy functional is determined by the lowest eigenvalue λ of the *fluctuation matrix* M. As explained in Supplementary Notes [15], λ can be obtained from the iterative solution of DMFT equations. The difference of the Green's functions in iterations n and $n+1$ of the DMFT self-consistency loop is given by

$$\delta G^{(n+1)}(i\omega_n) - \delta G^{(n)}(i\omega_n) = e^{-n\lambda} \delta G^{(0)}(i\omega_n) \qquad (3)$$

and therefore λ determines the rate of convergence of the Green function to its solution.

An example of our calculations is shown in the inset of Fig. 2, where the eigenvalues at several temperatures are plotted as a function of interaction U/U_c. The minima of these curves define the locus of the "*instability trajectory*" $U^\star(T)$, which terminates at the critical end-point (U_c, T_c), as shown on Fig. 2. Note, that the immediate vicinity $T \approx T_c$ of the critical end-point has been carefully studied theoretically [3], and even observed in experiments [2], revealing classical Ising scaling (since one has a finite temperature critical point) of transport in this regime. In our study, we examine the crossover behavior at much higher temperatures $T \gg T_c$, displaying very different behavior: precisely what is expected in presence of *quantum criticality*.

Resistivity calculation. To reveal quantum critical scaling, we calculate the temperature dependence of the resistivity along a set of trajectories parallel to our instability trajectory (fixed $\delta U = U - U^\star(T)$). Resistivity was calculated using standard DMFT procedures [1], with the

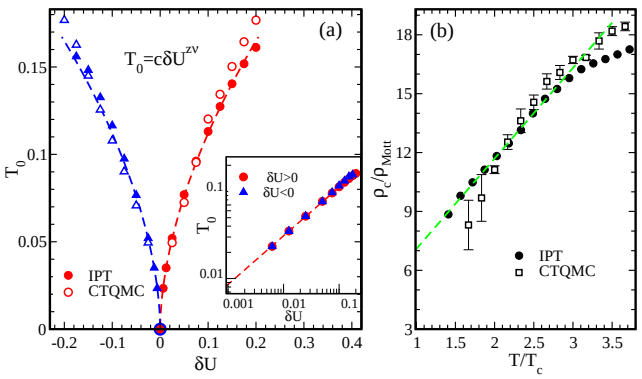

Figure 3: (Color online) (a) Scaling parameter $T_0(\delta U)$ as function of control parameter $\delta U = U - U^\star$; the inset illustrates power-law dependence of scaling parameter $T_0 = c|\delta U|^{z\nu}$; (b) Resistivity $\rho_c(T)$ of the "separatrix". Excellent agreement is found between IPT (closed symbols) and CTQMC (open symbols) results.

maximum entropy method [16] utilized to analytically continue CTQMC data to the real axis. The resistivity results are shown in Fig. 1, where on panel (a) IPT resistivity data for $\delta U = 0, \pm 0.025, \pm 0.05, \pm 0.1, \pm 0.15, \pm 0.2$ in the temperature range of $T \approx 0.07 - 0.2$ are presented (CTQMC data are not shown for the sake of clarity of the figure). The resistivity is given in units of ρ_{Mott}, maximal resistivity according to the Boltzmann quasi-classical theory of transport [17]. The family of resistivity curves above ($\delta U > 0$) the "separatrix" $\rho_c(T)$ (dashed line, corresponding to $\delta U = 0$) has an insulating-like behavior, while metallic dependence is obtained for $\delta U < 0$.

Scaling analysis. According to what is generally expected for quantum criticality, our family of curves should satisfy the following scaling relation:

$$\rho(T, \delta U) = \rho_c(T) f(T/T_o(\delta U)). \qquad (4)$$

We thus first divide each resistivity curve by the "separatrix" $\rho_c(T) = \rho(T, \delta U = 0)$ and then rescale the temperature, for each curve, with an appropriately chosen parameter $T_0(\delta U)$ to collapse our data onto two branches, Fig. 1(b). Note that this unbiased analysis *does not assume* any specific form of $T_o(\delta U)$: it is determined for each curve simply to obtain optimum collapse of the data [18]. This puts us in a position to perform a stringent test of our scaling hypothesis: true quantum criticality corresponds to $T_o(\delta U)$ which vanishes at $\delta U = 0$ and displays power law scaling with the same exponents for both scaling branches. As seen in Fig. 3(a) T_0 falls sharply as $U = U^\star$ is approached, consistent with the QC scenario, but opposite to what is expected in a "classical" phase transition. The inset of Fig. 3(a) with log-log scale shows clearly a power-law behavior of $T_0 = c|\delta U|^{z\nu}$, with the estimated power $(z\nu)^{IPT}_{\delta U<0} = 0.56 \pm 0.01$ for "metallic " side, and $(z\nu)^{IPT}_{\delta U>0} = 0.57 \pm 0.01$ for an insulating branch.

We also find (Fig. 3(b)) a very unusual form of our critical resistivity $\rho_c(T)$, corresponding to the instability trajectory. Its values largely exceeds the Mott limit, yet it displays metallic-like but non-Fermi liquid-like temperature dependence $\rho_c(T) \sim T$. Such puzzling behavior, while inconsistent with any conventional transport mechanism, has been observed in several strongly correlated materials close to the Mott transition [17, 20]. Our results thus suggest that it represents a generic feature of Mott quantum criticality.

$\beta-$function and mirror symmetry of scaled curves. To specify the scaling behavior even more precisely, we compute the corresponding β-function [4] $\beta(g) = \frac{d \ln g}{d \ln T}$, with $g = \rho_c/\rho$ being the inverse resistivity scaling function. Remarkably (Fig. 4(a)), it displays a nearly linear dependence on $\ln g$, and is continuous through $\delta U = 0$ indicating precisely the same form of the scaling function on both sides of the transition - another feature exactly of the form expected for genuine quantum criticality. This functional form is very natural for the insulating transport, as it is obtained even for simple activated behavior $\rho(T) \sim e^{-E_g/T}$. The fact that the same functional form *persists* well into the metallic side is a surprise, especially since it covers almost an order of magnitude for the resistivity ratio. Such a behavior has been interpreted [4] to reflect the "strong coupling" nature of the critical point, which presumably is governed by the same physical processes that dominate the insulator. This points to the fact that our QC behavior has a strong coupling, i.e. non-perturbative character.

The fact that the $\beta-$function assumes this logarithmic form on both sides of the transition is mathematically equivalent [4] to stating that the two branches of the corresponding scaling functions display "mirror symmetry" over the same resistivity range. Indeed, we find that transport in this QC region exhibits a surprisingly developed reflection symmetry (dash vertical lines of Fig. 4(a) mark its boundaries). Such a symmetry is clearly seen in Fig. 4(b), where the resistivity ρ/ρ_c (for $\delta U > 0$) and conductivity $\sigma/\sigma_c = \rho_c/\rho$ ($\delta U < 0$) can be mapped onto each other by reflection with $\frac{\rho(\delta U)}{\rho_c} = \frac{\sigma(-\delta U)}{\sigma_c}$ [21]. Note that $T/T_o = 1$ sets the boundary of the quantum critical region, over which the reflection symmetry of scaled curves is observed. It is depicted by dash-dotted crossover lines T_0 on phase diagram of Fig. 2 [15].

These remarkable features of the $\beta-$function, and associated reflection-symmetry, have been observed earlier in experimental [1, 21] and theoretical [4] studies, which tentatively associated this with disorder-dominated MITs. Speculation that $\beta \sim \ln g$ reveals disorder as the fundamental driving force for MIT, presumably reflects the fact that, historically, it has first been recognized for Anderson transitions [5]. Our work, however, shows that such behavior can be found even in absence of disorder - in interaction driven MITs. This finding calls for re-thinking of basic physical processes that can drive the MIT.

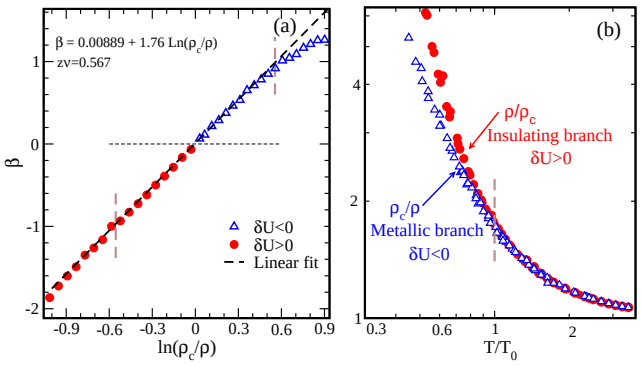

Figure 4: (Color online) (a) $\beta-$function shows linear in $\ln(\rho_c/\rho)$ behavior close to the transition. Open symbols are for metallic branch ($\delta U < 0$) and closed ones are for the insulating side ($\delta U > 0$) ; vertical dashed lines indicate the region where mirror symmetry of curves is found. (b) Reflection symmetry of scaled curves close to the transition.

Conclusions: We have presented a careful and detailed study of incoherent transport in the high temperature crossover regime above the critical endpoint T_c of a single-band Hubbard model. Our analysis revealed a so-far overlooked scaling behavior of the resistivity curves, which we interpreted as evidence of "hidden" Mott quantum criticality. Precisely locating the proposed QCP in our model is hindered by presence of the low temperature coexistence dome, which limits our quantum critical scaling to the region well above T_c. Regarding the nature of transport in the QC regime, we found that the critical resistivity well exceeds the Mott limit, and yet it - surprisingly - assumes a metallic form, in dramatic contrast to conventional MIT scenarios. These features, together with large amounts of entropy characterizing this entire regime [22], prove surprisingly reminiscent of the "holographic duality" scenario [23, 24] for a yet-unspecified QC point. Interestingly, the holographic duality picture has - so far - been discussed mostly in the context of quantum criticality in correlated metals (e.g. $T = 0$ magnetic transitions in heavy fermion compounds). Ours is the first work proposing that the same physical picture could apply to quantum criticality found at the MIT.

We believe that our results provide a significant new perspective on QC around the Mott transition, and a deeper understanding of an apparent universality in the high temperature crossover regime. Our method traces a clear avenue for further searches for QC scaling, which are likely to be found in many other regimes and models.

In particular, it would be interesting to study a corresponding critical regime by going beyond the single-site DMFT analysis. It was shown in [19] that inclusion of spatial fluctuations does not significantly modify the high temperature crossover region in half-filled Hubbard model. Consequently, we expect our main findings to persist. An even more stringent test of our ideas should be provided in models where the critical end-point T_c can be significantly reduced. This may include studies of the Mott transition away from half-fillling [25], or in systems with frustrations [6, 26]. In such situations the proposed scaling regime should extend to much lower temperatures, perhaps revealing more direct evidence of the - so far - hidden Mott QC point. Our ideas should also be tested by performing more detailed transport experiments in the relevant incoherent regime, a task that may be easily accessible in various organic Mott systems [3], where T_c is sufficiently below room temperature.

The authors thank K. Haule for the usage of his CTQMC code, and M. Jarrell for the use of his Maximum Entropy code for analytical continuation of the CTQMC data. This work was supported by the National High Magnetic Field Laboratory and the NSF through grants DMR-0542026 and DMR-1005751 (H.T. and V.D.), and Serbian Ministry of Science under project No. ON171017 (J.V. and D.T.). D.T. acknowledges support from the NATO Science for Peace and Security Programme grant No. EAP.RIG.983235. Numerical simulations were run on the AEGIS e-Infrastructure, supported in part by FP7 projects EGI-InSPIRE, PRACE-1IP and HP-SEE.

[1] E. Abrahams *et al.*, Rev. Mod. Phys. **73**, 251 (2001).
[2] P. Limelette *et al.*, Science **302**, 89 (2003).
[3] F. Kagawa *et al.*, Nature **436**, 534 (2005).
[4] V. Dobrosavljević *et al.*, Phys. Rev. Lett. **79**, 455 (1997).
[5] E. Abrahams *et al.*, Phys. Rev. Lett. **42**, 673 (1979).
[6] A. Camjayi *et al.,* Nature Phys. **4**, 932 (2008).
[7] A. Georges *et al.*, Rev. Mod. Phys. **68**, 13 (1996).
[8] P. Werner *et al.*, Phys. Rev. Lett. **97**, 076405 (2006).
[9] K. Haule, Phys. Rev. B **75,** 155113 (2007).
[10] G. Kotliar, *et al.*, Phys. Rev. Lett. **48**, 5180 (2000).
[11] M. J. Rozenberg *et al.*, Phys. Rev. Lett. **75**, 105 (1995).
[12] J. H. Mooij, Phys. Status Solidi, A **17**, 521 (1973).
[13] G. Moeller *et al.*, Phys. Rev. B **59**, 6846 (1999).
[14] M. J. Case and V. Dobrosavljević, Phys. Rev. Lett. **99**, 147204 (2007).
[15] See supplementary notes for eigenvalue analyis and scaling procedure.
[16] M. Jarrell and J.E. Gubernatis, Physics Reports **269**, 133, (1996).
[17] N. E. Hussey *et al.*, Philos. Mag. 84, 2847 (2004).
[18] Other criteria have also been emplyed to identify a MIT crossover line. [19] used the flatness of the lowest Matsubara points of the self-energy, [1, 11] used the inflection point of the resistivity curves. We have not reveal any apparent scaling behavior following these trajectories.
[19] H. Park *et al.*, Phys. Rev. Lett. **101**, 186403 (2008).
[20] B. J. Powell and R. H. McKenzie, J. Phys.: Condens. Matter 18, R827 (2006).
[21] D. Simonian *et al.*, Phys. Rev. B. **55**, 13 421 (1997).
[22] L. De Leo *et al.*, arXiv:1009.2761v1 (2010).
[23] S. Sachdev, Phys. Rev. Lett. **105**, 151602 (2010).
[24] J. McGreevy, Physics **3**, 83 (2010).
[25] G. Sordi *et al.*, Phys. Rev. B **80**, 035129 (2009).
[26] M. Eckstein *et al.*, Phys. Rev. B. **75**, 125103 (2007).

SUPPLEMENTARY NOTES: QUANTUM CRITICAL TRANSPORT NEAR THE MOTT TRANSITION

Eigenvalue analysis of the free energy curvature

Here we present in detail the procedure that we use to determine the minimum curvature of the free energy functional for a given temperature. For simplicity we concentrate on the Bethe lattice. The Ginzburg-Landau free energy functional $F(\vec{G})$ in the Hilbert space of the Matsubara Green's functions $\vec{G} \equiv G(i\omega_n)$ is given by [1–3]

$$\begin{aligned} F(\vec{G}) &= -Tt^2\vec{G}^2 + F_{imp}(\vec{G}) \\ &= -Tt^2 \sum_n G^2(i\omega_n) + F_{imp}(\vec{G}), \end{aligned} \tag{5}$$

where the first term is the energy cost of forming the Weiss field $\vec{\Delta} = t^2\vec{G}$ around a given site, while the second term is the free energy of an electron at this site in the presence of the Weiss field.

Close to a local extremum $\vec{G}_0$, we can Taylor expand $F(\vec{G})$ in terms of deviation from this point $\delta\vec{G} = \vec{G} - \vec{G}_0$:

$$\begin{aligned} F(\vec{G}) &= F(\vec{G}_0) + Tt^2 \sum_{mn} \delta G(i\omega_m) M_{mn} \delta G(i\omega_n) + \dots \\ &= F(\vec{G}_0) + Tt^2\, \delta\vec{G}\hat{M}\delta\vec{G} + \dots \end{aligned} \tag{6}$$

where

$$M_{mn} = \frac{1}{2Tt^2} \frac{\partial^2 F(\vec{G})}{\partial G(i\omega_n)\partial G(i\omega_m)}\bigg|_{\vec{G}=\vec{G}_0}. \tag{7}$$

We introduce a gradient function

$$\vec{g}(\vec{G}) \equiv \frac{1}{2Tt^2}\frac{\partial F(\vec{G})}{\partial \vec{G}} = \hat{M}\delta\vec{G} \tag{8}$$

and define an iteration-substitution procedure by

$$\delta\vec{G}^{(n+1)} = \delta\vec{G}^{(n)} - \vec{g}(\vec{G}^{(n)}), \tag{9}$$

which gives the minimum of the free energy as the iteration step $n \to \infty$. In the case of the free energy functional given by Eq. (5), we have

$$\vec{g}(\vec{G}) = \vec{G}_{imp}(\vec{G}) - \vec{G}, \tag{10}$$

and in the iterative procedure the Green's function converges to the minimum of the free energy which is at the same time also a self-consistent solution of the DMFT equations, given by the relation $G_{imp}(i\omega_n) = G(i\omega_n)$.

The curvature of the free energy for interaction U and temperature T can be obtained as follows. The eigenbasis $\vec{G}_\alpha$ and eigenvalues λ_α of matrix $\hat{M}$ are defined by

$$\hat{M}\vec{G}_\alpha = \lambda_\alpha \vec{G}_\alpha. \tag{11}$$

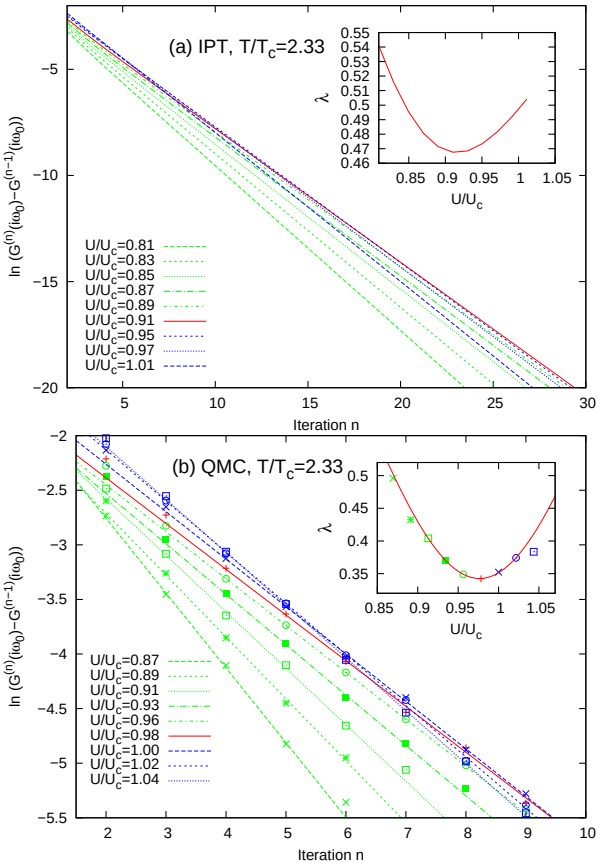

Figure 5: Convergence rate in the iterative solution of DMFT equations at $T/T_c = 2.33$ using IPT impurity solver, panel (a), and CTQMC impurity solver, panel (b). The dashed lines in panel (b) are linear fits to the data. The insets are the corresponding eigenvalues determined by the slopes from the main panels.

We can expand $\delta\vec{G}^{(n)}$ as

$$\delta\vec{G}^{(n)} = \sum_\alpha a_\alpha^{(n)} \vec{G}_\alpha \tag{12}$$

where $a_\alpha^{(n)}$ are the coefficients of $\delta\vec{G}^{(n)}$ in the eigenvalue basis. Substituting into Eq. (9), one obtains

$$\delta\vec{G}^{(n)} = \sum_\alpha e^{-nB_\alpha} a_\alpha^{(0)} \vec{G}_\alpha, \tag{13}$$

where

$$B_\alpha = -\ln(1-\lambda_\alpha). \tag{14}$$

For large n the term with lowest $B_\alpha = B_{\alpha_0}$, which corresponds to the lowest eigenvalue $\lambda_{\alpha_0} \equiv \lambda$, is dominant

$$\delta\vec{G}^{(n)} = e^{-nB_{\alpha_0}} a_{\alpha_0}^{(0)} \vec{G}_{\alpha_0}, \quad n \gg 1. \tag{15}$$

Here α_0 is the coefficient corresponding to the Green function with the lowest eigenvalue λ. Now it is obvious that through iterations, the solution $\vec{G}$ approaches to $\vec{G}_0$

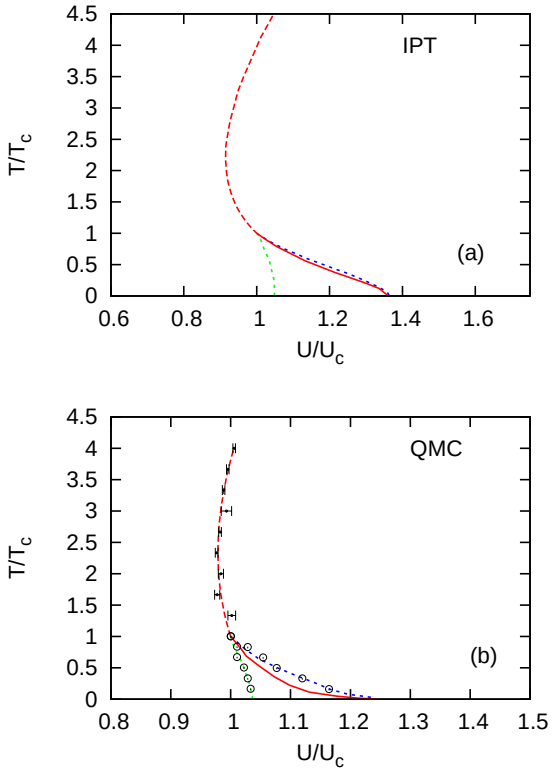

Figure 6: Phase diagram obtained with IPT, panel (a), and CTQMC, panel (b). Temperature and interaction are scaled by their values at the critical endpoint ($T_c^{IPT} = 0.046$, $T_c^{QMC} = 0.03$ and $U_c^{IPT} = 2.472$, $U_c^{QMC} = 2.3$). Red dashed line is the instability line $U^*(T)$, full red line is the line of the first order MIT, and green and blue dotted lines are left and right spinodals.

exponentially along a direction defined by the eigenvector of $\hat{M}$ corresponding to its minimal eigenvalue λ. The coefficient B_{α_0} and the corresponding eigenvalue λ are then obtained from the slope in the iterative relation

$$\ln\left[G(i\omega_n)^{(n+1)} - G(i\omega_n)^{(n)}\right] = const - nB_{\alpha_0}, \quad (16)$$

which follows from Eq. (13).

In practice, to obtain λ (and thus the curvature of free energy), we monitor DMFT loop convergence rate, $G(i\omega_o)^{(n+1)} - G(i\omega_o)^{(n)}$, in as many iterations as possible and then linearly fit $\ln\left(G(i\omega_o)^{(n+1)} - G(i\omega_o)^{(n)}\right)$ versus iteration index n. Here $\omega_o = \pi T$ is the lowest Matsubara frequency. For small λ, $B_{\alpha_0} \approx \lambda$. We repeat this procedure for different values of U at the same temperature T to determine $U^*(T)$ in which $\lambda(U)|_T$ is minimal. It takes few iterations of the DMFT loop to enter into the linear regime given by Eq. (16).

With IPT impurity solver, we can use data from several tens of iterations to determine the slope B_{α_0}, Fig. 1(a). The solution with CTQMC impurity solver has a statistical error and the number of iterations is limited before the

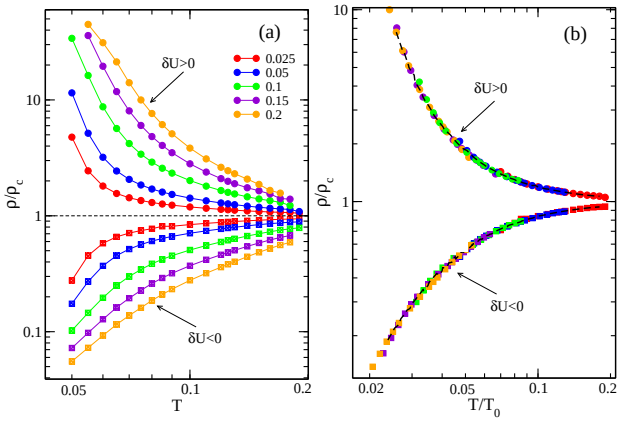

Figure 7: (a) Resistivity as function of temperature for $\delta U = \pm 0.025, 0.05, 0.1, 0.15, 0.2$. (b) By scaling the data along $T-$axis by T_0 data are collapsed onto two branches. Data are collapsed on the lowest $\delta U = \pm 0.025$ curves.

difference $|G(i\omega_o)^{(n+1)} - G(i\omega_o)^{(n)}|$ becomes too small and acquires a large relative statistical error. Nevertheless, we were able to determine rather precisely the eigenvalue λ and the interaction $U^*(T)$ for which it becomes minimal, Fig. 1(b). The "instability line" corresponding to the minimum curvature of the free energy is shown in Fig. 2(a) (IPT phase diagram), and Fig. 2(b) (CTQMC phase diagram). Error bars in Fig. 2(b) are estimates of the uncertainty in the position of the instability line.

Details of the scaling procedure

The resistivity $\rho(T, \delta U)$ is calculated along the lines parallel to the instability line $U^*(T)$. Here $\delta U = U - U^*(T)$. The resistivity is fist divided by its value $\rho_c(T)$ at $\delta U = 0$, Fig. 3(a). Then for each δU the temperature axis is scaled by T_0 where the scaling parameter T_0 is chosen to collapse the data onto two branches: insulating-like for $\delta U > 0$ and metallic-like for $\delta U < 0$. The scaling was done in such a way that data were collapsed on the lowest curves with $\delta U = \pm 0.025$ as shown in Fig. 3(b). The scaling parameter T_0 has a power law form $T_0 = c|\delta U|^{z\nu}$, where the prefactor c depends on this referent value of U.

Our data exhibit a reflection symmetry which is seen in Fig. 4(a), where the resistivity ρ/ρ_c (for $\delta U > 0$) and conductivity $\sigma/\sigma_c = \rho_c/\rho$ ($\delta U < 0$) can be mapped onto each other by reflection with $\frac{\rho(\delta U)}{\rho_c} = \frac{\rho_c(-\delta U)}{\rho}$.

The standard estimate for the scale (prefactor) of the crossover temperature is obtained by requiring that the scaling variable $x = T/T_0 = 1$ at the point where the scaling function changes its functional form; in our case this corresponds to the temperature below which the mirror symmetry of the scaling curves no longer holds. Before rescaling the prefactor, this is found at

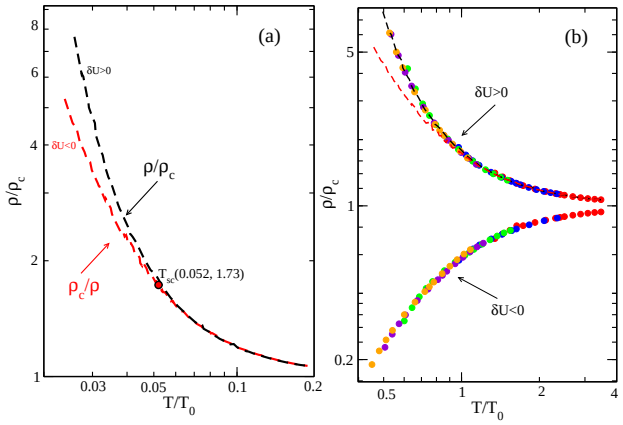

Figure 8: (a) Total scaled data (for clarity shown by single branches) exhibit reflection symmetry for $T \geq T_{sc}$. (b) T/T_0-axis is rescaled by T_{sc} in such a way that $T/T_o = 1$ set the boundary of quantum critical region over which the reflection symmetry of scaled curves is observed.

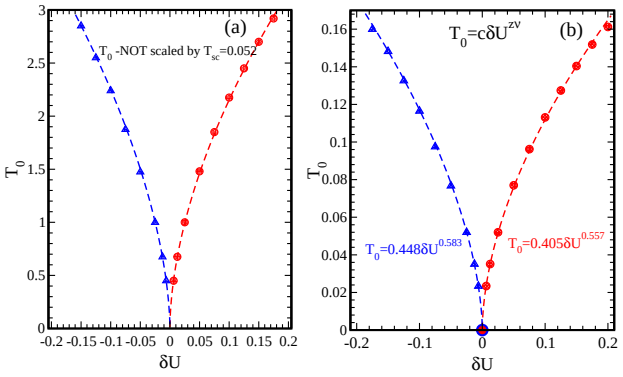

Figure 9: (a) Scaling temperature T_0 vs. δU obtained from scaling procedure shown on Fig. 4(a). (b) T_0 vs. δU after rescaling by T_{sc}. The boundary of the quantum critical region is now given by condition $T/T_o = 1$.

$x^* = T_{sc}/T_o = 0.052$. Our final form of scaled data is shown in Fig. 4(b), where T/T_0 - axis is rescaled by $x^* = T_{sc}/T_o$ so that $T/T_o = 1$ sets the *boundary of the quantum critical region*. The scaling parameter T_0 as function of δU is shown in Fig. 5(a) (before rescaling with x^*) and in Fig. 5(b) (after rescaling with x^*). The corresponding values for c and $z\nu$ from the power law fit are also given.

We can now plot the crossover temperature T_0 setting the boundary of QC region on our phase diagram. $T = T_0$ condition is equivalent to

$$T_0 = c|\delta U(T_o)|^{\nu z} = c\delta|U - U^\star(T_o)|^{z\nu}, \qquad (17)$$

where $U^\star(T_o)$ is value of U at temperature $T = T_o$, along the instability line. This equation implicitly defines the crossover line $T_o(U)$. Alternatively, we can invert this dependence to describe the same crossover line as $U_0(T)$ that takes the form

$$U_o^{\pm}(T) = U^\star(T) \pm (T/c)^{1/z\nu}. \qquad (18)$$

As we can see from this expression, the crossover line approaches the instability line at low T and diverges away from it at high T. The phase diagram including the instability line and the crossover temperature T_0 is shown on Fig. 6.

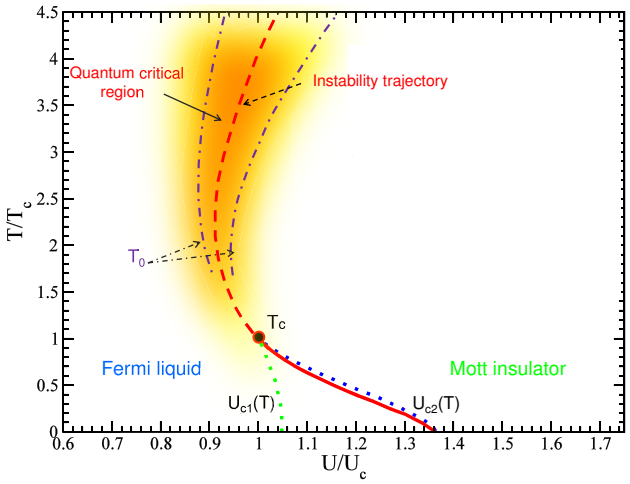

Figure 10: (Color online) DMFT phase diagram of the fully frustrated half-filled Hubbard model. The thick dashed line, which extends at $T > T_c$ shows the "instability trajectory" $U^*(T)$, and the crossover temperature T_o delimits the QC region (dash-dotted lines).

[1] A. Georges, G. Kotliar, W. Krauth, and M. J. Rozenberg, Rev. Mod. Phys. **68**, 13 (1996).

[2] G. Moeller, V. Dobrosavljević, and A. E. Ruckenstein, Phys. Rev. B **59**, 6846 (1999).

[3] G. Kotliar, E. Lange and M. J. Rozenberg, Phys. Rev. Lett. **48**, 5180 (2000).